Chemistry in Disks.
(Research Note)

IV. Benchmarking gas-grain chemical models with surface reactions.

D. Semenov[1], F. Hersant[2,3], V. Wakelam[2,3], A. Dutrey[2,3], E. Chapillon[4], St. Guilloteau[2,3], Th. Henning[1], R. Launhardt[1], V. Piétu[5], and K.Schreyer[6]

[1] Max Planck Institute for Astronomy, Königstuhl 17, D-69117 Heidelberg, Germany e-mail: `semenov@mpia.de`
[2] Université de Bordeaux, Observatoire Aquitain des Sciences de l'Univers, 2 rue de l'Observatoire, BP 89, F-33271 Floirac Cedex, France
[3] CNRS, UMR 5804, Laboratoire d'Astrophysique de Bordeaux, 2 rue de l'Observatoire, BP 89, F-33271 Floirac Cedex, France
[4] Max-Planck-Institut für Radioastronomie, Auf dem Hügel 69, D-53121 Bonn, Germany
[5] IRAM, 300 rue de la piscine, F-38406 Saint Martin d'Hères, France
[6] Astrophysikalisches Institut und Universitäts-Sternwarte, Schillergässchen 2-3, D-07745 Jena, Germany

ABSTRACT

Context. We detail and benchmark two sophisticated chemical models developed by the Heidelberg and Bordeaux astrochemistry groups.
Aims. The main goal of this study is to elaborate on a few well-described tests for state-of-the-art astrochemical codes covering a range of physical conditions and chemical processes, in particular those aimed at constraining current and future interferometric observations of protoplanetary disks.
Methods. We consider three physical models: a cold molecular cloud core, a hot core, and an outer region of a T Tauri disk. Our chemical network (for both models) is based on the original gas-phase osu_03_2008 ratefile and includes gas-grain interactions and a set of surface reactions for the H-, O-, C-, S-, and N-bearing molecules. The benchmarking is performed with the increasing complexity of the considered processes: (1) the pure gas-phase chemistry, (2) the gas-phase chemistry with accretion and desorption, and (3) the full gas-grain model with surface reactions. Using atomic initial abundances with heavily depleted metals and hydrogen in its molecular form, the chemical evolution is modeled within 10^9 years.
Results. The time-dependent abundances calculated with the two chemical models are essentially the same for all considered physical cases and for all species, including the most complex polyatomic ions and organic molecules. This result however required a lot of efforts to make all necessary details consistent through the model runs, e.g. definition of the gas particle density, density of grain surface sites, the strength and shape of the UV radiation field, etc.
Conclusions. The reference models and the benchmark setup, along with the two chemical codes and resulting time-dependent abundances are made publicly available in the Internet. This will facilitate and ease the development of other astrochemical models, and provide to non-specialists a detailed description of the model ingredients and requirements to analyze the cosmic chemistry as studied, e.g., by (sub-) millimeter observations of molecular lines.

Key words. astrochemistry – stars: formation – molecular processes – ISM: molecules, abundances

1. Introduction

Astrochemistry plays an important role in our understanding of the star- and planet-formation processes across the Universe (e.g., Bergin et al., 2007; Kennicutt, 1998; Solomon & Vanden Bout, 2005; van Dishoeck & Blake, 1998). Molecules serve as unique probes of physical conditions, evolutionary stage, kinematics and chemical complexity. In astrophysical objects molecular concentrations are usually hard to predict analytically as it involves a multitude of chemical processes that almost never reach a chemical steady-state. Consequently, to calculate molecular concentrations one has to specify initial conditions and abundances, and solve a set of chemical kinetics equations.

Since the first seminal studies on chemical modeling of the interstellar medium (ISM) by Bates & Spitzer (1951), Herbst & Klemperer (1973), and Watson & Salpeter (1972), numerous chemical models of molecular clouds (e.g., Hasegawa et al., 1992), protoplanetary disks (e.g., Aikawa et al., 2002), shells around late-type stars (e.g., Agúndez & Cernicharo, 2006), AGN tori (e.g., Meijerink et al., 2007), and planetary atmospheres (e.g., Gladstone et al., 1996) have been developed. These models are mainly based on three widely applied ratefiles: the UDFA (Umist Database For Astrochemistry[1]) (Millar et al., 1997; Le Teuff et al., 2000; Woodall et al., 2007), the OSU database (Ohio State University[2]) (Smith et al., 2004), and a network incorporated in the "Photo-Dissociation Region" code from Meudon[3] (Le Petit et al., 2006). Recently another database of chemical

---

[1] `http://www.udfa.net`
[2] `http://www.physics.ohio-state.edu/~eric/research.html`
[3] `http://aristote.obspm.fr/MIS/pdr/charge.html`

reactions for the interstellar medium and planetary atmospheres, KIDA[4], has been opened to the astrochemical community. The main aim of KIDA is to group all kinetic data to model the chemistry of these environments and to allow physico-chemists to upload their data to the database and astrochemists to present their models. Several compilations of surface reactions have also been presented (e.g., Allen & Robinson, 1977; Tielens & Hagen, 1982; Hasegawa et al., 1992; Hasegawa & Herbst, 1993; Garrod & Herbst, 2006). The detailed physics and chemistry processes incorporated in the modern theoretical models allow to predict and, at last, to fit the observational interferometric data such as, e.g., molecular line maps of protoplanetary disks and molecular clouds (e.g., Semenov et al., 2005; Dutrey et al., 2007; Goicoechea et al., 2009; Panić & Hogerheijde, 2009; Henning et al., 2010b). However, with the advent of forthcoming high-sensitivity, high-resolution instruments like ALMA, ELT, and JWST, the degree of complexity of these models will have to be increased and their foundations to be critically re-evaluated to match the quality of the data (e.g., Asensio Ramos et al., 2007; Lellouch, 2008; Semenov et al., 2008).

There are other difficulties with cosmochemical models. Apart from often poorly known physical properties of the object, its chemical modeling suffer from uncertainties of the reaction rates, of which only $\lesssim 10\%$ have been accurately determined (see, e.g., Herbst, 1980; Wakelam et al., 2006; Vasyunin et al., 2008). In contrast to these internal uncertainties, another major source of ambiguity is the lack of detailed description of chemical models that often incorporate different astrochemical ratefiles, initial abundances, dust grain properties, etc., thus making results hard to interpret and compare. It is thus essential to perform consistent benchmarking of various advanced chemical models under a variety of realistic physical conditions, in particular those encountered in protoplanetary disks. To the best of our knowledge, the only important benchmarking study attempted so far focused on several PDR physico-chemical codes (Röllig et al., 2007).

The ultimate goal of present work is i) to provide a detailed description of our time-dependent sophisticated chemical codes and ii) to establish a set of reference models covering a wide range of physical conditions, from a cold molecular cloud core to a hot corino and an outer region of a protoplanetary disk. In comparison with the PDR benchmark, our study is based on a more extended set of gas-grain and surface reactions. All the relevant software, figures, reaction network, and calculated abundances are available in the Internet[5].

The organization of the paper is the following. In Section 2, the two codes and the chemical network are presented in detail, along with our approach to calculate the reaction rates. In Section 3, we describe various benchmarking models, the physical conditions, and the initial chemical abundances. The benchmarking runs and their results are presented and compared in Section 4. Final conclusions are drawn in Section 5.

2. Chemical Models

2.1. Heidelberg and Bordeaux chemical codes

In this study, we compare two chemical codes, "ALCHEMIC" and "NAUTILUS", developed independently over the last several years by the Heidelberg and Bordeaux astrochemistry groups. Both codes have been intensively utilized in various studies of molecular cloud and protoplanetary disk chemistry, e.g. the influence of the reaction rate uncertainties on the results of chemical modeling of cores (Vasyunin et al., 2004; Wakelam et al., 2005, 2006) and disks (Vasyunin et al., 2008), modeling of the disk chemical evolution with turbulent diffusion (Semenov et al., 2006; Hersant et al., 2009), interpretation of interferometric data (Semenov et al., 2005; Dutrey et al., 2007; Schreyer et al., 2008; Henning et al., 2010a), and predictions for ALMA (Semenov et al., 2008). Both codes are optimized to model time-dependent evolution of a large set of gas-phase and surface species linked through thousands of gas-phase, gas-grain and surface processes. We found that both these codes have comparable performance, accuracy, and fast convergence speed thanks to the use of advanced ODE and sparse matrix linear system solvers.

The Heidelberg "ALCHEMIC" code is written in Fortran 77 and based on the publicly available DVODPK (Differential Variable-coefficient Ordinary Differential equation solver with the Preconditioned Krylov method GMRES for the solution of linear systems) ODE package[6]. The full Jacobi matrix is generated automatically from the supplied chemical network to be used as a left-hand preconditioner. For astrochemical models dominated by reactions involving hydrogen, the Jacobi matrix is sparse (having $\lesssim 1\%$ of non-zero elements), so to solve the corresponding linearized system of equations a high-performance sparse unsymmetric MA28 solver from the Harwell Mathematical Software Library[7] is used. As ratefiles, both the recent OSU 06 and osu.2008 and the RATE 06 networks can be utilized. A typical run with relative and absolute accuracies of 10^{-5} and 10^{-15} for the full gas-grain network with surface chemistry (~ 650 species, $\sim 7\,000$ reactions) and 5 Myr of evolution takes only a few seconds of CPU time on the Xeon 2.8GHz PC (with gfortran 4.3 compiler).

The Bordeaux "NAUTILUS" code is written in Fortran 90 and uses the LSODES (Livermore Solver for Ordinary Differential Equations with general Sparse Jacobian matrix) solver, part of ODEPACK[8] (Hindmarsh, 1983). "NAUTILUS" is adapted from the original gas-grain model of Hasegawa & Herbst (1993) and its subsequent evolutions made over the years at the Ohio State University. The main differences with the OSU model rely in the numerical scheme and optimization ("NAUTILUS" is about 20 times faster), the possibility to compute 1D structures with diffusive transport and the adaptation to disk physics and chemistry. The full Jacobian is computed from the chemical network without preconditioning. For historical reasons, only the OSU rate files are being used, although minor adjustments could permit to extend the model to other networks. Similar performances with "ALCHEMIC" are achieved, the same typical run of the full gas-grain network taking a few seconds on a standard desktop computer.

Below we detail how we model various gas-phase and surface reactions.

---

[4] `http://kida.obs.u-bordeaux1.fr`
[5] `http://www.mpia.de/homes/semenov/Chemistry_benchmark/home.html`
[6] `http://www.netlib.org/ode/vodpk.f`
[7] `http://www.hsl.rl.ac.uk/`
[8] `http://www.netlib.org/odepack/`

2.2. Modeling of Chemical Processes

Chemical codes solve numerically the equations of chemical kinetics describing the formation and destruction of molecules:

$$\frac{dn_i}{dt} = \sum_{l,m} k_{lm} n_l n_m - n_i \sum_{i \neq l} k_l n_l + k_i^{\text{des}} n_i^s - k_i^{\text{acc}} n_i \tag{1}$$

$$\frac{dn_i^s}{dt} = \sum_{l,m} k_{lm}^s n_l^s n_m^s - n_i^s \sum_{i \neq l} k_l^s n_l^s - k_i^{\text{des}} n_i^s + k_i^{\text{acc}} n_i \tag{2}$$

where n_i and n_i^s are the gas-phase and surface concentrations of the i-th species (cm^{-3}), k_{lm} and k_l are the gas-phase reaction rates (in units of s^{-1} for the first-order kinetics and cm^3 s^{-1} for the second-order kinetics), k_i^{acc} and k_i^{des} denote the accretion and desorption rates (s^{-1}), respectively, and k_{lm}^s and k_l^s are surface reaction rates (cm^3 s^{-1}).

2.2.1. Gas-phase reactions

For the benchmarking purposes, we utilize a recent osu_03_2008 gas-phase ratefile[9]. This ratefile incorporates the data for the 456 atomic, ionic, and molecular species involved in the 4389 gas-phase reactions. The corresponding reaction rates are calculated as follows, using the standard Arrhenius representation:

$$k(T) = \alpha \left(\frac{T}{300} \right)^\beta \exp\left(-\frac{\gamma}{T} \right), \tag{3}$$

where α is the value of the reaction rate at the room temperature of 300 K, the parameter β characterizes the temperature dependence of the rate, and γ is the activation barrier (in Kelvin). We utilize this expression for all gas-phase two-body processes, e.g. ion-molecular and neutral-neutral reactions.

For the cosmic ray and FUV ionization and dissociation the following prescriptions have been used.

Cosmic ray (CR) ionization & dissociation

$$k_{\text{CR}} = \alpha \zeta_{\text{CR}}, \tag{4}$$

where $\zeta_{\text{CR}} = 1.3 \, 10^{-17}$ s^{-1} is the adopted CR ionization rate. In all benchmarking models any additional sources of ionization like the X-ray stellar radiation and the decay of short-living radionucleides (e.g., ^{26}Al and ^{40}K) are not considered. This small set of reactions includes ionization of relevant atoms and dissociation of molecular hydrogen. The same expression is used to compute photodissociation and ionization by the CR-induced FUV photons. Also, the CR- and UV-driven dissociation of surface species is calculated by the Eq. 4 (616 processes).

FUV photodissociation & ionization
To calculate photoreaction rates through the environment, we adopt pre-computed fits of van Dishoeck (1988) for a 1D plane-parallel slab, using the Draine FUV IS radiation field. Unlike in the PDR benchmarking study, the self- and mutual-shielding of CO and H$_2$ against UV photodissociation are not taken into account for simplicity. The corresponding rate is calculated as:

$$k_{\text{FUV}} = \alpha \exp\left(-\gamma A_{\text{V}}\right) \chi, \tag{5}$$

9 http://www.physics.ohio-state.edu/~eric/research.html

where the A_{V} is the visual extinction (mag.) and the χ is the unattenuated FUV flux expressed in units of the FUV interstellar radiation field χ_0 of Draine (1978). We do not take the Ly$_\alpha$ radiation into account as it requires sophisticated modeling of the radiation transport – a full-scale benchmarking study by itself (e.g., Pascucci et al., 2004; Röllig et al., 2007).

2.3. Gas-grain interactions

For simplicity, we assume that the dust grains are uniform spherical particles, with a radius of $a_g = 0.1 \, \mu m$, made of amorphous olivine, with density of $\rho_d = 3$ g cm^{-3} and a dust-to-gas mass ratio $m_{d/g} = 0.01$. The surface density of sites is $N_s = 1.5 \, 10^{15}$ sites cm^{-2}, and the total number of sites per such a grain is $S = 1.885 \, 10^6$. The dust and gas temperatures are assumed to be the same.

Gas-grain interactions start with the accretion of neutral molecules onto dust surfaces with a sticking efficiency of 100% (195 processes). Molecules are assumed to only physisorb on the grain surface (by van der Waals force) rather than by forming a chemical bond with the lattice (chemisorption). The rate of accretion of a gas-phase species i (cm^{-3} s^{-1}) is given by:

$$R_{\text{acc}}(i) = k_{\text{acc}}(i) n(i), \tag{6}$$

where $n(i)$ is the density of gas-phase species i (cm^{-3}), and $k_{\text{acc}}(i) = \sigma_d \langle v(i) \rangle n_d$ is the accretion rate. Here $\sigma_d = \pi a_g^2$ is the geometrical cross section of the grain with the radius a_g, n_d is the density of grains (cm^{-3}) and $\langle v(i) \rangle$ is the thermal velocity of species i (cm s^{-1}). The latter quantity is expressed as $\sqrt{8 k_B T / (\pi \mu(i) m_p)}$, with T being the gas temperature (K), $m_p = 1.66054 \, 10^{-24}$ g is the proton's mass, $\mu(i)$ is the reduced mass of the molecule i (in atomic mass units), and $k_B = 1.38054 \, 10^{-16}$ erg K^{-1} is the Boltzmann's constant. All constants are summarized in Table 2.

In addition, electrons can stick to neutral grains, producing negatively charged grains. Atomic ions radiatively recombine on these negatively charged grains, leading to grain neutralization (13 reactions in total). The corresponding two-body reaction rate is calculated as:

$$k(T) = \alpha \left(\frac{T}{300} \right)^\beta \frac{n_{\text{H}}}{n_d}, \tag{7}$$

where n_{H} is the total hydrogen nucleus density (cm^{-3}). This quantity is calculated by the following expression:

$$n_{\text{H}} = \frac{\rho}{\mu m_p}, \tag{8}$$

where ρ is the gas mass density (g cm^{-3}), and $\mu = 1.43$ is the mean mass per hydrogen nucleus. Consequently, the density of grains n_d is expressed as:

$$n_d = \frac{\rho m_{d/g}}{4/3 \pi a_g^3 \rho_d \mu}. \tag{9}$$

We consider neither interactions of molecular ions with grains nor the photoelectric effect leading to positively charged grains.

In our simplified model used for benchmarking purposes, the surface molecules can leave the grain by only two mechanisms. First, they can desorb back into the gas phase when a grain is hit by a relativistic iron nucleus and heated for a short while up to several tens of Kelvin (160 reactions, cosmic-ray induced

desorption). Second, in sufficiently warm regions thermal desorption becomes efficient. The thermal desorption for the *i*-th surface molecule is calculated by the Polanyi-Wigner equation:

$$k_{\mathrm{des}}(T_d) = \nu(i) \exp\left(-\frac{E_{\mathrm{des}}}{T_d}\right). \tag{10}$$

Here $\nu(i) = \sqrt{\frac{2N_s k_B E_{\mathrm{des}}}{\pi^2 m m_p}}$ is the characteristic vibrational frequency of the *i*-th species, E_{des} is its desorption energy (Kelvin), *m* the mass of the species and T_d is the grain temperature. Desorption energies E_{des} are taken from Garrod & Herbst (2006). We do not distinguish between various thermal evaporation scenarios for different molecules, e.g. via "volcanic" or multilayer desorption (Collings et al., 2004).

The cosmic ray desorption rate is computed as suggested by Eq. 15 in Hasegawa & Herbst (1993). It is based on the assumption that a cosmic ray particle (usually an iron nucleus) deposits on average 0.4 MeV into a dust grain of the adopted radius, impulsively heating it to a peak temperature $T_{\mathrm{crp}} = 70$ K (see also Leger et al., 1985). The resulting rate is:

$$k_{\mathrm{crd}} = f k_{\mathrm{des}}(70\ K) \tag{11}$$

k_{crd} is the thermal evaporation rate at 70 K times the fraction of time the grain temperature stays close to 70 K. The fraction *f* is a ratio of a grain cooling timescale via desorption of molecules to the timescale of subsequent heating events (e.g., for a 0.1μm silicate particle and the standard CR ionization rate $1.3\ 10^{-17}$ s^{-1} these timescales are $\sim 10^{-5}$ s and $\sim 3\ 10^{13}$ s, respectively). Other non-thermal desorption mechanisms that can play an important role in chemistry of protoplanetary disks like photodesorption are not considered.

2.4. Surface Reactions

Surface reactions (532 in the network) are treated in the standard rate approximation, assuming only Langmuir-Hinshelwood formation mechanism, as described, e.g., in Hasegawa et al. (1992). Surface species are only allowed to move from one surface site to another by thermal hopping. When two surface species find each other, they can recombine. We assume that the products do not leave the surface as the excess of energy produced by such a reaction will be immediately absorbed by the grain lattice, i.e. we did not include the desorption process proposed by Garrod et al. (2007).

Rate coefficients for surface reactions between species *i* and *j* are expressed as follows:

$$k_{i,j} = P(R_{\mathrm{diff}}(i) + R_{\mathrm{diff}}(j))/n_d. \tag{12}$$

Here *P* is the probability for the reaction to occur. This parameter is 1 for an exothermic reaction without activation energy and 1/2 if the two reactants are of the same type. For exothermic reactions with activation energy E_a (or endothermic reactions), this probability is $\alpha \exp\left(-\frac{E_a}{T}\right)$, with α the branching ratio of the reaction ($\alpha = 1/3$ if there are three reaction channels). In some cases, tunneling effects can increase this probability[10]. When this is the case, *P* is computed through the following formula (Hasegawa et al., 1992):

$$P = \alpha \exp[-2(b/\hbar)(2k_B \mu(i) m p E_a)^{1/2}] \tag{13}$$

---

[10] This process is not included in ALCHEMIC and thus has not been tested in this benchmark.

with *b* the barrier thickness (1 Å) and $\hbar$ the Planck constant times 2π (1.05459×10^{-27} erg s^{-1}).

The thermal diffusion rate of species *i* is:

$$R_{\mathrm{diff}}(i) = \nu(i) \exp(-\frac{T_{\mathrm{diff}}(i)}{T_d})/S. \tag{14}$$

Here $k_B T_{\mathrm{diff}}$ is the activation energy of diffusion for the *i*-th molecule.

The diffusion and desorption energies of a limited set of molecular species have been derived (e.g., Katz et al., 1999; Bisschop et al., 2006; Öberg et al., 2007). Moreover, these energies depend on the type of the surface lattice and its structural properties (porosity, crystallinity) (e.g., Acharyya et al., 2007; Thrower et al., 2009). While diffusion energy of a species must be lower than its desorption energy, the exact ratio is not well constrained for a majority of molecules in our network (except for H_2, see Katz et al., 1999). Following Ruffle & Herbst (2000), we adopted the $T_{\mathrm{diff}}/T_{\mathrm{des}}$ ratio of 0.77 for the all relevant species in the model.

It has been proposed that light surface species like H, H_2 and isotopes can also quantum tunnel through a potential well of the surface site and thus be able to quickly scan the surface, greatly increasing the efficiency of surface recombination even at very low temperatures (e.g., Duley & Williams, 1986; Hasegawa et al., 1992). However, according to the theoretical interpretation of Katz et al. (1999) tunneling of atomic hydrogen on amorphous surfaces does not occur. Therefore, it is not considered in our benchmarking study.

Finally, at very low influx of reacting species having a high recombination rate, concentrations on a grain can become very low, leading to a stochastic regime. In this case surface chemistry cannot be reliably described by the standard rate equation method, which tends to overestimate the rates. Other approaches like Monte Carlo techniques (e.g., Vasyunin et al., 2009), master equations (e.g., Green et al., 2001), and modified rate equations (e.g., Caselli et al., 1998; Garrod et al., 2009) should then be utilized. As it has been shown by Vasyunin et al. (2009), this only happens for rather dilute, warm gas and very small grains, and when quantum tunneling of hydrogen is allowed. Thus, the use of the standard rate equation approach to model surface chemistry is fully justified in our benchmarking study.

2.5. Initial abundances & other parameters

We use an up-to-date set of elemental abundances from Wakelam & Herbst (2008). The 12 elemental species include H, He, N, O, C, S, Si, Na, Mg, Fe, P and Cl. Except for hydrogen, which is assumed to be entirely locked in molecular form, all elements are initially atomic. They are also ionized except for He, N and O (see Table 3). All heavy elements are heavily depleted from the gas phase similar to the "low metals" abundances of Lee et al. (1998). All grains are initially neutral. Since large-scale chemical models with an extended set of surface reactions rarely reach a chemical steady state, all benchmarking tests run over a long evolutionary time span of 10^9 years (with 60 logarithmic time steps, starting from 1 year). Both chemical codes use the same absolute and relative accuracy parameters for the solution, 10^{-20} and 10^{-6}, respectively.

3. Benchmarking models

The physical conditions of the five benchmarking cases are summarized in Table 1, (see also Snow & McCall, 2006;

Hassel et al., 2008). These are chosen to represent realistic astrophysical object yet to be relatively simple. We decide to focus first on physical models representative of less complex astrophysical media: a cold core ("TMC1") and a hot corino ("HOT CORE"). The "TMC1" model has a temperature of 10 K, a hydrogen nucleus density of 2×10^4 cm^{-3}, and a visual extinction of 10 mag. The "HOT CORE" model has a temperature of 100 K, a hydrogen nucleus density of 2×10^7 cm^{-3}, and a visual extinction of 10 mag. Both models have FUV IS RF $\chi = 1\chi_0$ of Draine (1978) and $\zeta_{CR} = 1.3 \, 10^{-17}$ s^{-1}.

Protoplanetary disks are more complex objects from chemical point of view. Basically, an outer disk ($r \gtrsim 50 - 100$ AU) observable with modern radio-interferometers can be divided in three distinct parts from top to bottom. The hot and tenuous disk surface (usually called "disk atmosphere") is located at above 4-6 gas scale heights. In this region disk chemistry is similar to that of HII and PDR region, with a limited set of primal ionization-recombination processes. There ionization is mainly governed by the stellar X-ray radiation and stellar and interstellar FUV radiation. Closer to the midplane, a partly X-ray and FUV-shielded region called the "warm molecular layer" is located (at about 1-3 scale heights). This mildly ionized, dense and warm layer is a harbor of complex chemistry, where gas-grain interactions and endothermic reactions are particularly active. There, a plethora of more complex species is formed and reside in the gas. Below is the highly dense, cold and dark midplane, where most molecules are frozen out onto grains, enabling a variety of slow surface processes to be active.

Instead of simulating disk chemistry in the entire disk, we decide to pick up a few representative disk regions with highly distinct physical conditions, and within the reach of spatial resolution of modern interferometers. We consider three representative layers taken at a radius of 98 AU (which requires a sub-arcsecond resolution even for nearby objects). Those are designated "DISK1" (the disk midplane), "DISK2" (the warm molecular layer), and "DISK3" (the disk atmosphere). We take physical conditions similar to those encountered in the DM Tau disk, for which a lot of high-resolution molecular data are available. In our simulations, we adopted the 1+1D steady-state irradiated disk model with vertical temperature gradient that represents the low-mass Class II protoplanetary disk surrounding the young T Tauri star DM Tau (D'Alessio et al., 1999). The disk has a radius of 800 AU, an accretion rate $\dot{M} = 10^{-8} \, M_\odot$ yr^{-1}, a viscosity parameter $\alpha = 0.01$, and a mass $M \simeq 0.07 \, M_\odot$ (Dutrey et al., 1997; Piétu et al., 2007). The central T Tau star has an effective temperature $T_* = 4\,000$ K, mass $M_* = 0.5 M_\odot$, and radius $R_* = 2R_\odot$.

We assumed that the disk is illuminated by the FUV radiation from the central star with an intensity $\chi = 410\,\chi_0$ at the distance of 100 AU and by the interstellar UV radiation with intensity χ_0 in plane-parallel geometry (Draine, 1978; van Dishoeck, 1988; Brittain et al., 2003; Dutrey et al., 2007). The visual extinction for stellar light at a given disk cell is calculated as:

$$A_V = \frac{N_H}{1.59 \cdot 10^{21}} \frac{\text{mag}}{\text{cm}^{-2}}, \tag{15}$$

where N_H is the vertical column density of hydrogen nuclei between the point and the disk atmosphere. Note that, according to our definition, the unattenuated stellar FUV intensity for a fixed disk radius is the largest in the midplane and gets lower for upper disk heights as the distance to the star increases.

Consequently, the "DISK1" model is located at 6.768 AU above the midplane, has a temperature of 11.4 K, a hydrogen nucleus density of 5.413×10^8 cm^{-3}, a visual extinction toward the star of 40.35 mag. and an extinction of 37.07 mag. in the

vertical direction, and the FUV RF intensity of $\chi_* = 428.3\chi_0$. The "DISK2" model is located at 29.97 AU above the midplane, has a temperature of 45.9 K, a hydrogen nucleus density of 2.588×10^7 cm^{-3}, a visual extinction toward the star of 23.23 mag. and the vertical extinction of 1.939 mag., and the FUV RF intensity of $\chi_* = 393.2\chi_0$. Finally, the "DISK3" cell is located at 45.44 AU above the midplane, has a temperature of 55.2 K, a hydrogen nucleus density of 3.669×10^6 cm^{-3}, a visual extinction toward the star of 1.608 mag. and the vertical extinction of 0.217 mag., and the FUV RF intensity of $\chi = 353.5\chi_0$. The remaining parameters of all the models are described above. All those parameters are summarized in Table 1.

4. Benchmarking Results

Using these 5 representative benchmarking models and our extended chemical network, time-dependent chemistry is calculated for the entire 10^9 years of evolution. A perfect agreement is achieved between the Bordeaux and Heidelberg chemical models for all considered physical conditions, all species, and all time moments. The results for assorted chemical species representing various chemical families and various degree of complexity are compared in Figs. 1–5. The good agreement is in fact not surprising when only chemistry is concerned. Both codes are based on the rate equations approach to model chemical processes and use well documented and robust procedures to handle a multitude of complex physico-chemical processes (e.g., photodissociation, cosmic ray desorption, photoprocessing of ices, surface reactions).

This agreement required all the constants, reaction rates, and parameters of the physical models between the two astrochemical codes to match perfectly. There are many important parameters not always mentioned in description of a chemical model, and which may hamper a comparison of results. In what follows, we discuss major problems that arose during course of our benchmarking study.

The first priority is to check that both codes have exactly the same values of fundamental constants expressed in the same physical units, and additional useful constants (e.g., year in seconds, UV albedo of the dust, etc.). Second, the "standard", well-defined physical parameters that can be defined as constants in the codes (like the cosmic ray ionization rate, the FUV IS, etc.) has to be checked. Our next major obstacle was different definition of gas particle density: one group uses pure hydrogen nucleus density while another uses mass density of the gas (with all heavy elements included). After we began to use the same units for the FUV radiation field and the same conversion factor between N_H and A_V our models showed perfect agreement for a pure gas-phase chemical network.

As a next point, we added gas-grain interactions to our models. After grain properties (shape, radius, density, surface density of sites, porosity, material, etc.) are fixed, apparently the best approach is to add reactions between atomic and molecular ions with charged grains, grain re-charging, and electron sticking to grains. Next, one has to adopt the value of the sticking coefficient of other gas-phase species. An unexpected issue at that stage came from the fact that "ALCHEMIC" used atomic masses including isotopes while "NAUTILUS" used atomic masses of major isotope only. Next, it is extremely important for disk chemical models under comparison to have similar desorption and diffusion energies of surface molecules since gas-grain interactions and build-up of thick complex icy mantles are powerful in protoplanetary disks. A substantial portion of time to reach the perfect agreement between the two models was spent

to properly implement desorption mechanisms. We did not consider UV photodesorption along with thermal and CRP-driven desorption because it would require a proper description of the UV radiation transport through the disk model. As we relied on the same rate equations approach for surface chemistry, the good agreement between the full models was reached soon. Here one has to be careful with treatment of homogeneous reactions (i.e., involving the same species, e.g. $H + H \rightarrow H_2$), as their rates by statistical arguments are only half of those for heterogeneous reactions. Last, but not least, for easy comparison of results it is important to specify in detail the output format of the simulated data.

5. Conclusion & Summary

We present in this paper the results of several detailed benchmarks of the two dedicated chemical codes for the Heidelberg and Bordeaux astrochemistry groups. Both codes are used to model time-dependent chemical evolution of molecular clouds, hot cores and corinos, and protoplanetary disks. The codes use the recent osu_03_2008 gas-phase ratefile, supplemented with an extended list of gas-grain and surface processes. A detailed description of the codes, along with considered chemical processes and means to compute their rates are presented. Five representative physical models are outlined, and their chemical evolution is simulated. The first case ("TMC1") is relevant to the chemistry of a dense cloud core, the second case ("Hot Corino") is similar to a warm star-forming region, e.g. an inner part of a hot core or corino. The last three models correspond to various disk layers at the radius of $\approx$ 100 AU, representing distinct chemistry. In all these benchmarking test runs, despite a large range of considered physical parameters like temperature of gas and dust, density, and UV intensity, we found perfect agreement between the codes. We however had to compare and bring into agreement step-by-step a large number of parameters and description of chemical processes in "ALCHEMIC" and "NAUTILUS". Moreover, this benchmark study allowed us to correct some minor errors and helped us to become fully confident in our chemical simulations and predictions. We hope that this study and detailed report on all components of the codes and models will be helpful for other astrochemical models to improve their quality. This is an essential step toward development of more sophisticated chemical models of the ISM and disks, since ALMA, the extremely powerful observational facility, will soon become operational. With this instrument, the quality of molecular interferometric maps will drastically improve, allowing observers and astrochemists to work together in order to investigate the chemistry of the planetary-forming zones in disks ($r < 30$ AU) in great detail.

References

Acharyya, K., Fuchs, G. W., Fraser, H. J., van Dishoeck, E. F., & Linnartz, H. 2007, A&A, 466, 1005
Agúndez, M. & Cernicharo, J. 2006, ApJ, 650, 374
Aikawa, Y., van Zadelhoff, G. J., van Dishoeck, E. F., & Herbst, E. 2002, A&A, 386, 622
Allen, M. & Robinson, G. W. 1977, ApJ, 212, 396
Asensio Ramos, A., Ceccarelli, C., & Elitzur, M. 2007, A&A, 471, 187

Bates, D. R. & Spitzer, L. J. 1951, ApJ, 113, 441
Bergin, E. A., Aikawa, Y., Blake, G. A., & van Dishoeck, E. F. 2007, in Protostars and Planets V, ed. B. Reipurth, D. Jewitt, & K. Keil, 751–766
Bisschop, S. E., Fraser, H. J., Öberg, K. I., van Dishoeck, E. F., & Schlemmer, S. 2006, A&A, 449, 1297
Brittain, S. D., Rettig, T. W., Simon, T., et al. 2003, ApJ, 588, 535
Caselli, P., Hasegawa, T. I., & Herbst, E. 1998, ApJ, 495, 309
Collings, M. P., Anderson, M. A., Chen, R., et al. 2004, MNRAS, 354, 1133
D'Alessio, P., Calvet, N., Hartmann, L., Lizano, S., & Cantó, J. 1999, ApJ, 527, 893
Draine, B. T. 1978, ApJS, 36, 595
Duley, W. W. & Williams, D. A. 1986, MNRAS, 223, 177
Dutrey, A., Guilloteau, S., & Guelin, M. 1997, A&A, 317, L55
Dutrey, A., Henning, T., Guilloteau, S., et al. 2007, A&A, 464, 615
Garrod, R. T. & Herbst, E. 2006, A&A, 457, 927
Garrod, R. T., Vasyunin, A. I., Semenov, D. A., Wiebe, D. S., & Henning, T. 2009, ApJ, 700, L43
Garrod, R. T., Wakelam, V., & Herbst, E. 2007, A&A, 467, 1103
Gladstone, G. R., Allen, M., & Yung, Y. L. 1996, Icarus, 119, 1
Goicoechea, J. R., Pety, J., Gerin, M., Hily-Blant, P., & Le Bourlot, J. 2009, A&A, 498, 771
Green, N. J. B., Toniazzo, T., Pilling, M. J., et al. 2001, A&A, 375, 1111
Hasegawa, T. I. & Herbst, E. 1993, MNRAS, 263, 589
Hasegawa, T. I., Herbst, E., & Leung, C. M. 1992, ApJS, 82, 167
Hassel, G. E., Herbst, E., & Garrod, R. T. 2008, ArXiv e-prints, 803
Henning, T., Semenov, D., Guilloteau, S., et al. 2010a, ArXiv e-prints
Henning, T., Semenov, D., Guilloteau, S., et al. 2010b, ApJ, 714, 1511
Herbst, E. 1980, ApJ, 241, 197
Herbst, E. & Klemperer, W. 1973, ApJ, 185, 505
Hersant, F., Wakelam, V., Dutrey, A., Guilloteau, S., & Herbst, E. 2009, A&A, 493, L49
Hindmarsh, A. C. 1983, in IMACS Transactions on Scientific Computation, Vol. 1, Scientific Computing, ed. R. S. Stepleman, 55–64
Katz, N., Furman, I., Biham, O., Pirronello, V., & Vidali, G. 1999, ApJ, 522, 305
Kennicutt, Jr., R. C. 1998, ARA&A, 36, 189
Le Petit, F., Nehmé, C., Le Bourlot, J., & Roueff, E. 2006, ApJS, 164, 506
Le Teuff, Y. H., Millar, T. J., & Markwick, A. J. 2000, A&AS, 146, 157
Lee, H.-H., Roueff, E., Pineau des Forets, G., et al. 1998, A&A, 334, 1047
Leger, A., Jura, M., & Omont, A. 1985, A&A, 144, 147
Lellouch, E. 2008, Ap&SS, 313, 175
Meijerink, R., Spaans, M., & Israel, F. P. 2007, A&A, 461, 793
Millar, T. J., Farquhar, P. R. A., & Willacy, K. 1997, A&AS, 121, 139
Öberg, K. I., Fuchs, G. W., Awad, Z., et al. 2007, ApJ, 662, L23
Panić, O. & Hogerheijde, M. R. 2009, A&A, 508, 707
Pascucci, I., Wolf, S., Steinacker, J., et al. 2004, A&A, 417, 793
Piétu, V., Dutrey, A., & Guilloteau, S. 2007, A&A, 467, 163
Röllig, M., Abel, N. P., Bell, T., et al. 2007, A&A, 467, 187
Ruffle, D. P. & Herbst, E. 2000, MNRAS, 319, 837
Schreyer, K., Guilloteau, S., Semenov, D., et al. 2008, A&A, 491, 821
Semenov, D., Pavlyuchenkov, Y., Henning, T., Wolf, S., & Launhardt, R. 2008, ApJ, 673, L195
Semenov, D., Pavlyuchenkov, Y., Schreyer, K., et al. 2005, ApJ, 621, 853
Semenov, D., Wiebe, D., & Henning, T. 2006, ApJ, 647, L57
Smith, I. W. M., Herbst, E., & Chang, Q. 2004, MNRAS, 350, 323
Snow, T. P. & McCall, B. J. 2006, ARA&A, 44, 367
Solomon, P. M. & Vanden Bout, P. A. 2005, ARA&A, 43, 677
Thrower, J. D., Collings, M. P., Rutten, F. J. M., & McCoustra, M. R. S. 2009, MNRAS, 394, 1510
Tielens, A. G. G. M. & Hagen, W. 1982, A&A, 114, 245
van Dishoeck, E. F. 1988, in ASSL Vol. 146: Rate Coefficients in Astrochemistry, ed. T. J. Millar & D. A. Williams, 49–82
van Dishoeck, E. F. & Blake, G. A. 1998, ARA&A, 36, 317
Vasyunin, A., Sobolev, A. M., Wiebe, D. Z., & Semenov, D. 2004, Astronomy Letters, 30, 566
Vasyunin, A. I., Semenov, D., Henning, T., et al. 2008, ApJ, 672, 629
Vasyunin, A. I., Semenov, D. A., Wiebe, D. S., & Henning, T. 2009, ApJ, 691, 1459
Wakelam, V. & Herbst, E. 2008, ArXiv e-prints, 802
Wakelam, V., Herbst, E., & Selsis, F. 2006, A&A, 451, 551
Wakelam, V., Selsis, F., Herbst, E., & Caselli, P. 2005, A&A, 444, 883
Watson, W. D. & Salpeter, E. E. 1972, ApJ, 174, 321
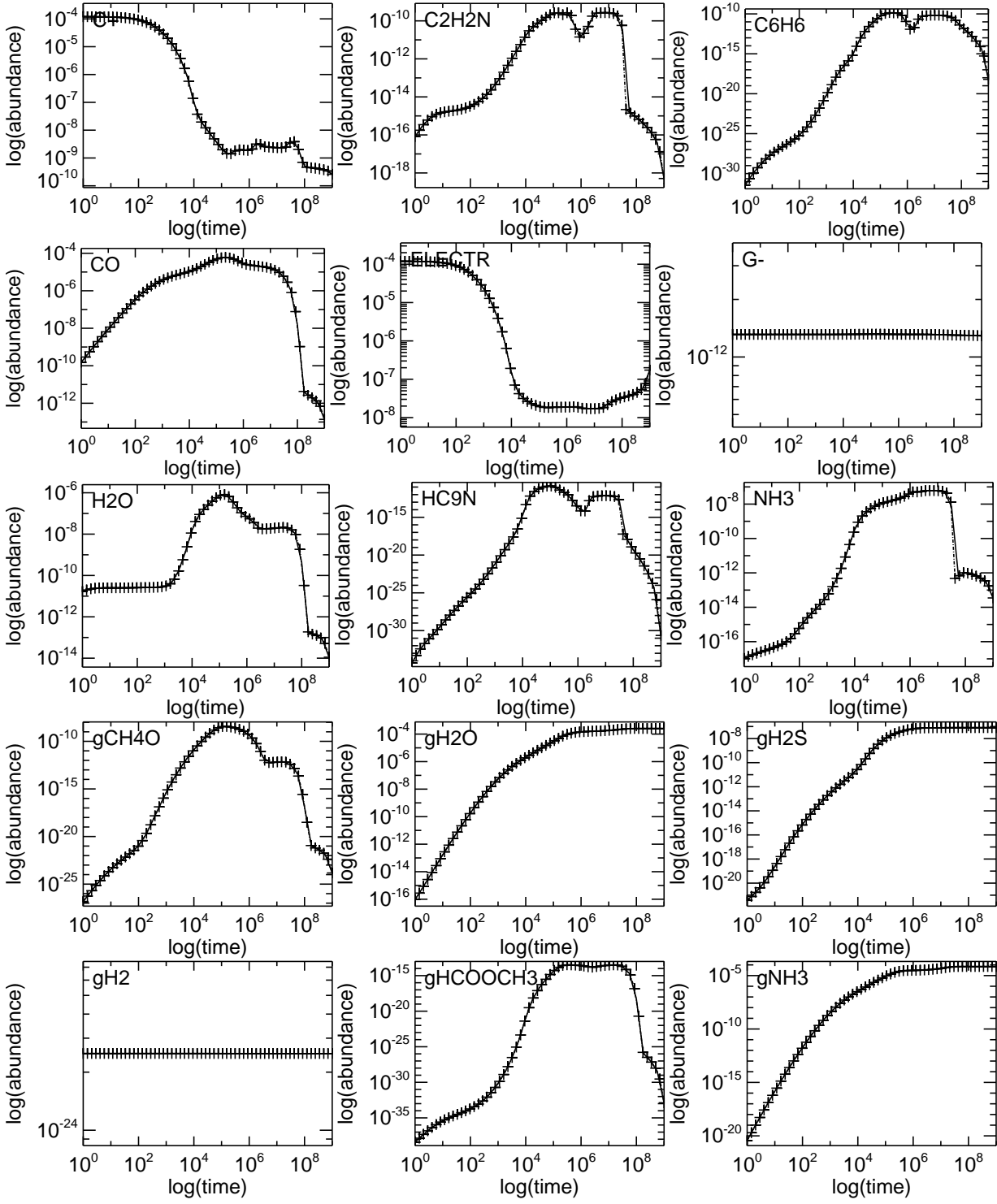Woodall, J., Agúndez, M., Markwick-Kemper, A. J., & Millar, T. J. 2007, A&A, 466, 1197

Fig. 1. Time-dependent abundances as computed with the Heidelberg (crosses) and Bordeaux (solid line) chemical models for the "TMC1" case. The X-axes show time in years. The Y-axes are abundances relative to the total amount of hydrogen nuclei. The species names are given in each panel. The prefix "g" denotes surface molecules, "CH4O" is methanol, and "G-" stands for negatively charged grains.
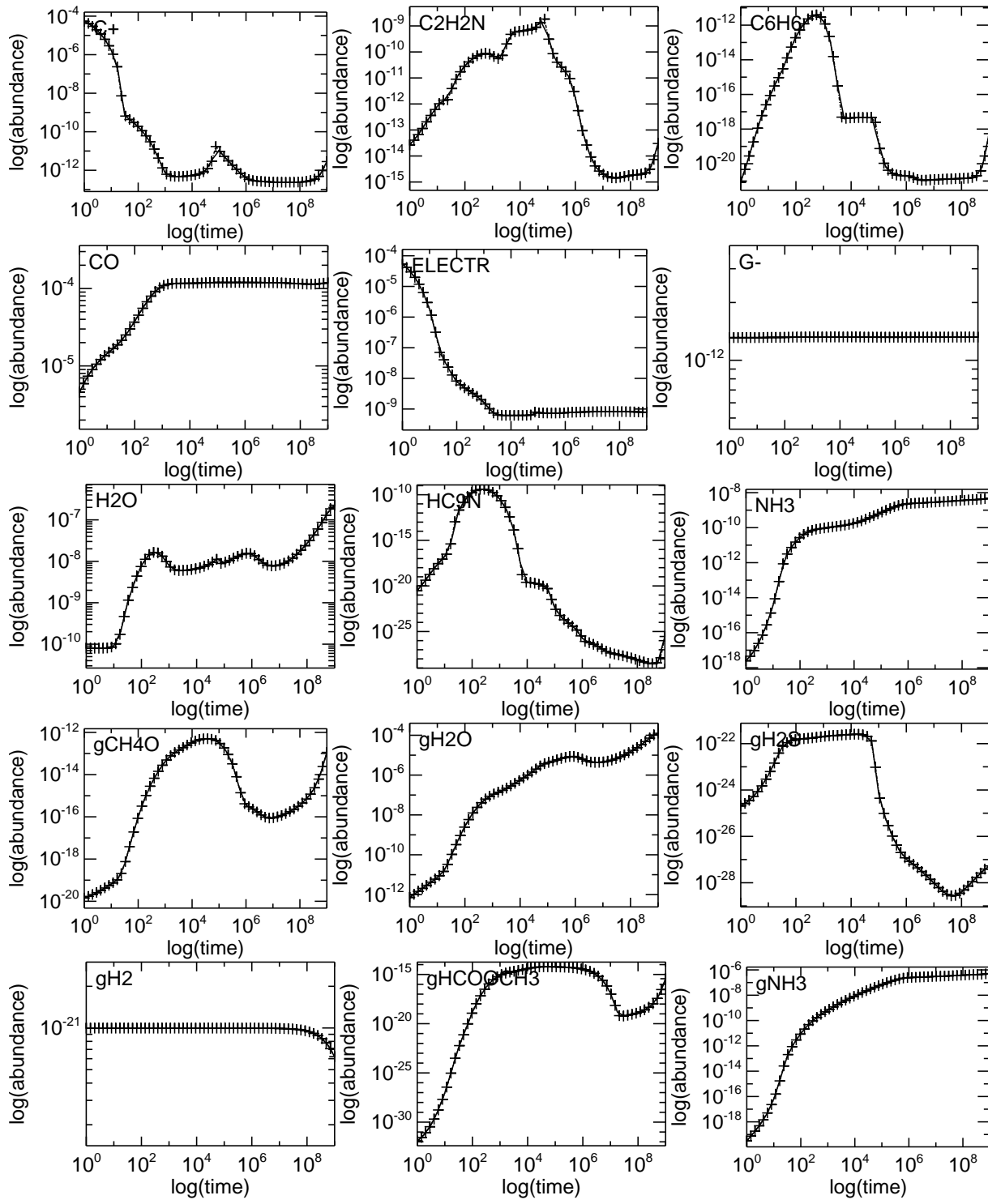
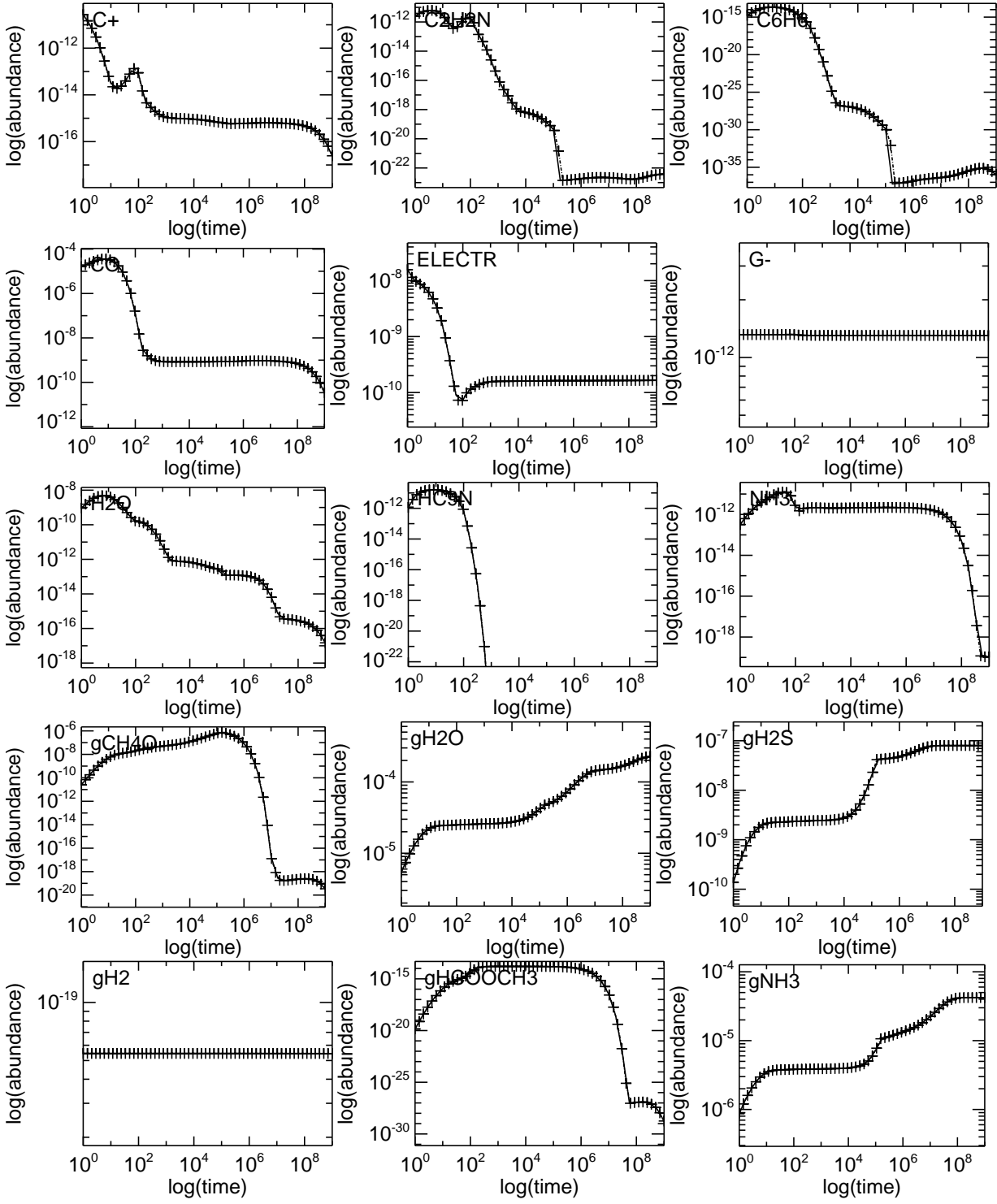**Fig. 2.** The same as in Fig. 1 but for the "Hot Corino" case.

Fig. 3. The same as in Fig. 1 but for the "DISK1" case (DM Tau, $r = 100$ AU, midplane).
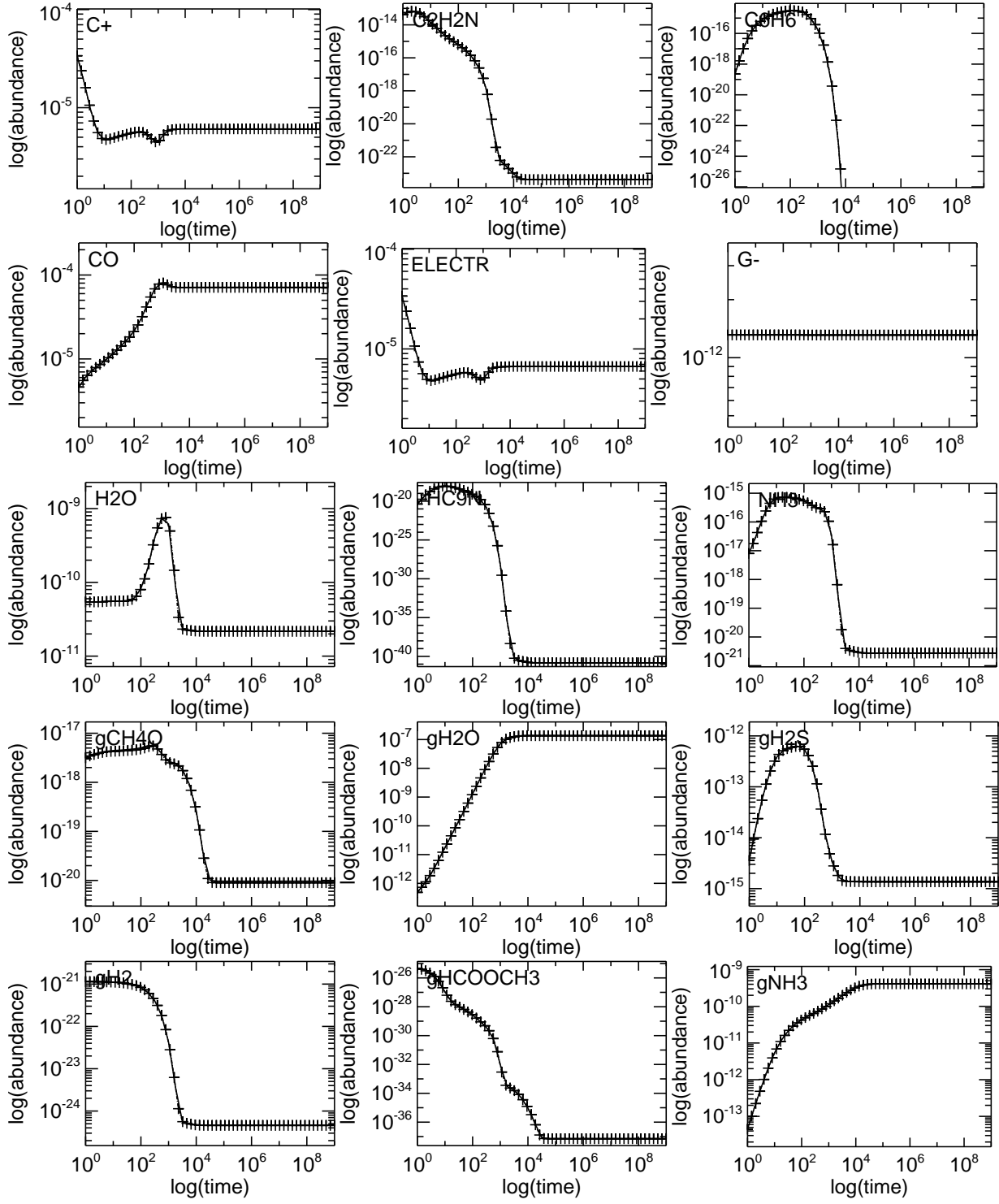
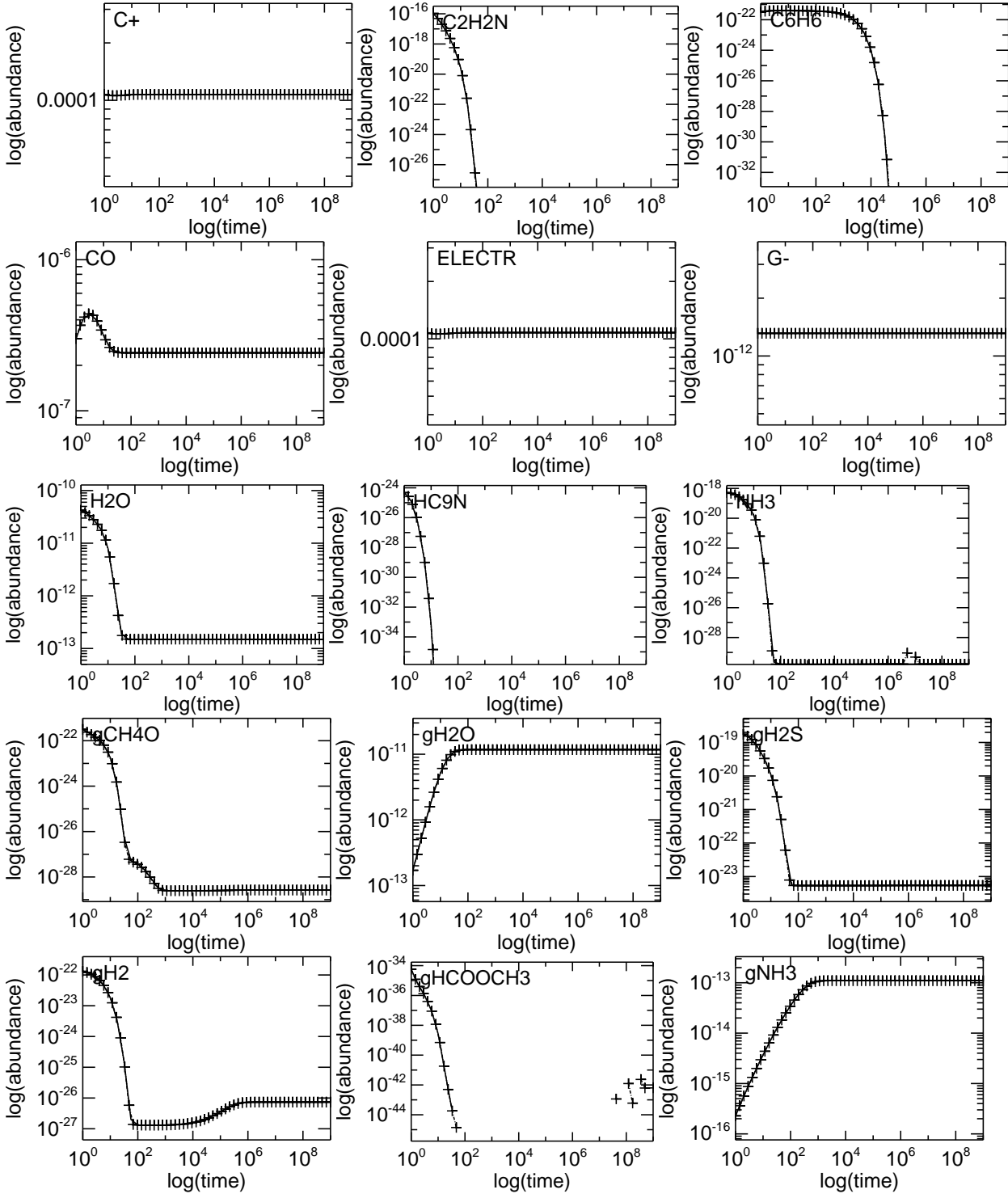**Fig. 4.** The same as in Fig. 3 but for the "DISK2" case (DM Tau, *r* = 100 AU, warm molecular layer).

Fig. 5. The same as in Fig. 3 but for the "DISK3" case (DM Tau, $r = 100$ AU, atmosphere).

Table 1. Physical models

Model	T	n(H+2H$_2$)	Av	χ [a]
	[K]	[cm^{-3}]	[mag]	
TMC1	10	2(4)[b]	10	χ_0
HOT CORE	100	2(7)	10	χ_0
DISK1	11.4	5.41(8)	37.1	428.3χ_0
DISK2	45.9	2.59(7)	1.94	393.2χ_0
DISK3	55.2	3.67(6)	0.22	353.5χ_0

[a] FUV, $6 < h\nu < 13.6$ eV, (Draine 1978)
[b] A(-B) means A$\times 10^{-B}$

Table 2. Constants and fixed parameters

Name	Value
k_B	1.38054×10^{-16} erg K^{-1}
$\hbar$	1.05459×10^{-27} erg s^{-1}
ζ_{CR}	1.3×10^{-17} s-1
a_g	0.1 μm
ρ_d	3 g cm^{-3}
$m_{d/g}$	0.01
N_S	1.5×10^{15} sites cm^{-2}
S	1.885×10^6
m_p	1.66054×10^{-24} g
μ	1.43 amu
T_{crp}	70 K
f	3×10^{-19}
b	1Å
$T_{\text{diff}}/T_{\text{des}}$	0.77

Table 3. Initial abundances

Species	$n(X)/n_{\text{H}}$
He	9.00(-2)[a]
H$_2$	5.00(-1)
C$^+$	1.2(-4)
N	7.6(-5)
O	2.56(-4)
S$^+$	8.00(-8)
Si$^+$	8.00(-9)
Na$^+$	2.00(-9)
Mg$^+$	7.00(-9)
Fe$^+$	3.00(-9)
P$^+$	2.00(-10)
CL$^+$	1.00(-9)

[a] A(-B) means A$\times 10^{-B}$